Mon. Not. R. Astron. Soc. **000**, 1–5 (1995) Printed 5 February 2008 (MN LaTeX style file v1.4)

Canada-France Redshift Survey X: The Quasar Sample

David Schade,[1,4] David Crampton[2,4] F. Hammer[3,4] O. Le Fèvre[3,4] S.J. Lilly[1,4]
[1] *Department of Astronomy, University of Toronto, 60 St. George St., Toronto, Canada M5S 1A7*
[2] *Dominion Astrophysical Observatory, National Research Council of Canada, Victoria, Canada*
[3] *DAEC, Observatoire de Paris-Meudon, 92195 Meudon, France*
[4] *Visiting Astronomer at the Canada-France-Hawaii Telescope which is operated by the National Research Council of Canada, the Centre National de la Recherche Scientifique de France, and the University of Hawaii.*

ABSTRACT

Six objects with broad emission lines and redshifts from 0.48 to 2.07 were discovered among 736 extragalactic objects in the Canada-France Redshift Survey (CFRS). Although the luminosities of half of the objects are such that they are in the Seyfert regime ($M_B > -23$), all would be designated as quasars in traditional surveys. Since the only selection criterion was that $17.5 \leq I_{AB} \leq 22.5$, or approximately $B < 23$ (assuming a continuum power-law slope $\alpha = -0.5$), these quasars represent an unbiased, flux-limited sample. Although uncertain, the implied surface density, 200^{+120}_{-80} deg^{-2} is the highest yet measured, and is in good agreement with extrapolations from other faint surveys and the evolving luminosity function models of Boyle (1991). The distributions of the continuum properties, emission-line strengths, etc., of the quasars do not differ significantly from those of quasars selected by other means, and therefore they would have been detected in most traditional surveys. Three of the quasars may be associated with clusters or large structures of galaxies at z > 1.

Key words: cosmology:observations—galaxies:morphology— quasars:luminosity function

1 INTRODUCTION

The Canada-France Redshift Survey (CFRS) is aimed at the detection of faint galaxies among objects with $17.5 \leq I_{AB} \leq 22.5$, with no discrimination against any other properties. The final catalog comprises 943 objects, of which 736 are extragalactic. The most common methods used to produce samples of quasars or active galactic nuclei (AGN) exploit their unusual colours, strong emission lines, variability, radio emission, X-ray emission, etc., and therefore are always biassed in some sense. Hewett and Foltz (1994) stress that if a completely unbiassed sample is not possible, an accurate assessment of the probability of detection as a function of absolute magnitude, redshift and spectral energy distribution must be made, and this is frequently lacking. Even though very effective and efficient survey techniques have been developed, there is always a danger that there may exist a subset of the population that might have been overlooked. Indeed, Webster(1995) has recently suggested that many more red quasars exist than previously supposed. Although the results of surveys based on techniques other than the popular UVX method can be examined to see if any such red population exists, surveys like CFRS can be considered as the ultimate check since spectroscopic observations are made for every object regardless of colour, morphology or spectroscopic properties. For example, the CFRS survey could detect red, radio-quiet, X-ray quiet quasars should they exist. On the other hand, since quasars constitute only $\sim 1\%$ of the surface density of objects on the sky at these magnitudes, CFRS cannot be expected to be an efficient survey for quasars.

The fundamental limit to CFRS as a quasar survey is the signal-to-noise at which a broad emission line object could be identified. In this paper, the properties of the six objects which would commonly be classified as quasars in major surveys are compared with those from other samples. Although distinction is often made between quasars and other AGNs, particularly Seyfert galaxies, such a distinction is not usually made in the basic surveys: any point-like object with strong, broad emission lines is usually classified as a quasar. Subsequently, further subdivisions are made based on luminosities and whether or not the object is extended under typical ground-based seeing conditions. In this paper, we adopt the traditional survey definition, and simply refer to all six strong emission line objects as quasars, partly to avoid confusion with other galaxies in our survey which

exhibit "AGN activity" in their nuclei (e.g., Tresse et al. 1994).

Our CFRS quasar sample, although very small, is relatively unique and hence it is of interest to compare it with samples derived by other methods. Colless et al. (1991) reported a similar analysis based on detection of two quasars in a faint blue-selected sample, $21 < b_J < 23.5$. Throughout this paper it is assumed that $H_\circ = 50$ km sec^{-1} Mpc^{-1} and $q_\circ = 0.5$.

2 OBSERVATIONS

As part of the Canada-France Redshift Survey, spectra were obtained of over 1000 objects with $17.5 \leq I_{AB} \leq 22.5$ in five different high galactic latitude fields selected to produce a fair sample of extragalactic objects (Lilly et al 1995a). The CFHT MOS spectrograph was used to cover the spectral region 4200 – 8600Å with a resolution of 7Å per CCD pixel, and slits were used which yielded a spectral resolution of FWHM ∼35Å. $BVIK$ photometry was also obtained for most objects in the spectroscopic sample (Lilly et al. 1995a). Details of all the observations, reduction techniques and sensitivity are presented by Le Fèvre et al. (1995a), Hammer et al. (1995), Lilly et al. (1995b) and Crampton et al. (1995). Eight one hour exposures were usually obtained of all targets so that spurious features such as cosmic rays were easily rejected, and features such as strong emission lines were readily apparent in all the individual spectra. The final CFRS catalog includes 591 galaxies with z < 1.3, 200 stars, 146 unidentified objects and 6 quasars. Colour and morphological information indicates that most of the unidentified objects are likely to be galaxies (Crampton et al. 1995) but 7 objects are quite compact and have colours not very different from the quasars. The minimum equivalent width of emission lines that would have been detected in the spectra of these seven objects is ∼30Å. Emission lines in the observed frame of at most a few percent of quasars at z > 2 would have been missed, if the equivalent width distributions of Francis et al. (1992) and Hartwick and Schade (1990) are assumed. The Mg II equivalent width distribution indicates that only ∼10% of low redshift (z < 1) quasars might have been missed, so it is unlikely that any quasars reside among the unidentified objects. Thus, only 6 quasars were detected among a total of 736 extragalactic objects. The total effective area surveyed was 112 arcmin^2.

Table 1 summarizes the properties of the quasars. The first column gives the CFRS number (the first two digits represent the right ascension of the field). The second and third columns give 2000 coordinates, followed by the isophotal I_{AB} magnitude ($I_{AB} = I + 0.48$), redshift, absolute magnitude, $(V-I)_{AB}$ colour, spectral index and rest-frame equivalent widths of strong emission lines. The errors of the equivalent widths are estimated to be ±10Å for most of the lines, and ±5Å for the lines of CFRS14.0198. Absolute magnitudes in the rest-frame B band were computed assuming a power-law continuum slope, $f_\nu = \nu^\alpha$, with α determined for each object from its $(V-I)_{AB}$ colour corrected for emission line contamination. As indicated above, not all of these "quasars" lie above the canonical division between quasars and Seyfert galaxies at $M_B = -23$ for ($H_\circ = 50$ km sec^{-1} Mpc^{-1}). It is interesting to note that no very high redshift quasars were discovered. Since our targets were selected by their I magnitudes, there is certainly no selection bias against high redshift quasars, and since Lyα would not disappear from our spectroscopic bandpass until z > 6, identification of high redshift quasars would have been straightforward had they been present. Spectra of the six quasars are presented in Figure 1 with the strongest emission lines marked. Finding charts from our deep I band images are given in Figure 2. At least three of the quasars may be in groups or large structures of galaxies, as noted below.

2.1 Notes on individual quasars

CFRS00.0207 z=1.352 is surrounded by many faint galaxies of similar magnitude; the five CFRS galaxies indicated in Figure 2 have isophotal $I_{AB} \sim 23.4 \pm 0.3$mag. It is conceivable that this quasar is embedded in a cluster similar to those recently proposed by Hutchings et al. (1994) and Matthews et al. (1994) around other z > 1 quasars.
CFRS03.0106 z=2.070 is 2.″3 from a ∼1.3 mag fainter galaxy.
CFRS03.0603 z=1.048 has a companion (615) only 16″ away which has identical redshift (1.048). In the larger CFRS field in this direction, there are three more galaxies with redshifts within Δz = 0.01 bringing the total to five. We have spectra of only one other object shown in the field; CFRS03.0602 is a star. The image of CFRS03.0603 appears to be slightly extended compared to the nearby stars, and the measured "compactness parameter", Q , (Le Fevre, et al. 1986) also indicates that it is resolved. Typically, CFRS point source objects have Q ≤1.3 (Crampton et al. 1995), while Q = 1.55 for this quasar. Since the absolute magnitude of this quasar is M= −23.0, it is at the border of the canonical Seyfert – quasar classification. Nevertheless, since z ∼1, it must reside in a bright host galaxy.
CFRS14.0198 z=1.6034: The bright object (163) is an M star.
CFRS14.1303 z=0.9859 appears to be part of a very large structure (spread over our entire field corresponding to 6.5 h_{50}^{-1} Mpc projected dimension for $q_\circ = 0$, and greater than 900 km/s in redshift space) containing an estimated 30 bright galaxies at z = 0.985 (Le Fèvre et al. 1994). The nearest of these is CFRS14.1262, only 17″ away. CFRS14.1275 is at z = 0.763 and CFRS 14.1327 is at z = 0.932. Strong lines of Ne III and Ne V are present in the spectrum of CFRS14.1303 (Fig. 1).
CFRS14.1567 z=0.4787 is slightly extended, indicating that the host galaxy is visible. Since M= −22.0, this quasar is more properly classified as a Seyfert. Only two of the nearby galaxies have redshifts measured; both 1525 and 1541 have z ∼0.74.

Even though there are indications that at least three of the quasars may be located in groups of galaxies, a more rigorous analysis (Le Fèvre et al 1995b) shows that only the group around 14.1303 is statistically significant.

3 DISCUSSION

3.1 Surface density

The effective area of the CFRS survey is 0.031 deg^2 so that the observed 6 quasars translate to a surface density of 200^{+120}_{-80} deg^{-2}; the highest surface density observed to date. The errors enclose a 1σ confidence interval (Gehrels 1986). The survey magnitude limit of I_{AB} $\leq$22.5 corresponds to $B = 23$ for quasars with a power-law spectral energy distribution ($f_\nu \propto \nu^\alpha$) with $\alpha = -0.5$.

For comparison, the previously-faintest quasar surveys reached a limiting magnitude of B $\sim$22. The Koo and Kron (1988) survey has a limiting magnitude of m$_J$=22.5 (B $\sim$m$_J + 0.1$), but spectroscopic followup has not yet been completed (Majewski, private communication). Zitelli et al. (1992, hereafter Z92) have surveyed 0.35 deg^2 to m$_J$ = 22 (and a smaller area to m$_J$=20.85). Their survey yields a quasar surface density at m$_J$=22 of 115$\pm$17 deg^{-2} and, for z$<$ 2.2, a surface density of 86$\pm$17 deg^{-2}. Boyle, Jones, and Shanks (1991) surveyed an area of 0.85 deg^2 to a similar limiting magnitude. Although their survey suffers from incompleteness for z $>$ 2.2 due to the UVX selection procedure, the surface density for quasars with z$<$2.2, 68$\pm$9 deg^{-2}, is in reasonable agreement with the Z92 result. In total, 118 new quasars were discovered in these two surveys. The Z92 result is also consistent with the surface density estimated in a review of all major surveys by Hartwick and Schade (1990). They derive a surface density of 160 quasars deg^{-2} at B = 22.5 and z $<$ 3.3 (or 129 at z $<$ 2.2) by applying a completeness correction to the work of Koo and Kron (1988). Figure 3 shows a comparison of all of these results for z $<$ 3.3. The surface density of quasars, log N $<$ B deg^{-2}, from Hartwick and Schade (1990) (circles) is combined with the newer results from Boyle et al. (1991) (open triangle) and Z92 (solid triangle). The faintest point (solid square) from the present survey lies on an extrapolation of the data from previous surveys, although the error bar is large.

An extrapolation of the Z92 quasar surface density using their slope of 0.40 for the log N versus M relation gives an expected number of 300 deg^{-2} at B = 23 for all redshifts, or 200 deg^{-2} at z $<$ 2.2. As noted above, although all of our quasars are at z $<$ 2.2, we clearly have no bias against objects at much larger redshifts. Our observed surface density of 200^{+120}_{-80} deg^{-2} is at most a mild contradiction to the extrapolation of the Z92 surface density in the sense that the expected number of low-redshift (z $<$ 2.2) objects is observed, but there is some deficit of high-redshift objects.

The faintest X-ray counts where optical identifications have been made are dominated by active galactic nuclei (Shanks et al 1991). Analysis of the deepest ROSAT counts yield surface density estimates of 413 X-ray sources deg^{-2} to a limiting flux of 2.5×10^{-15} erg cm^{-2} s^{-1} (Hasinger et al. 1993) and fluctuation analysis (Barcons et al. 1994) yields an estimate of 900 to 1800 discrete sources deg^{-2} brighter than 7×10^{-16} erg cm^{-2} s^{-1}. These counts (in the 0.5-2 KeV) band which might be taken as estimates of the quasar surface density are well above our own estimate.

3.1.1 Comparison with Boyle (1991) model

The expected number of quasars in various redshift bins (e.g, 0 $<$ z $<$ 0.5, 0.5 $<$ z $<$ 1.0, ...) can be computed from the model of Boyle et al. (1991). We find good agreement between the expectations derived from the evolving model and our observations. Over the range 0 $<$z$<$ 3 , 4.98 quasars are predicted by the model compared to 6 observed. The redshift distribution of the observed quasars also agrees well with the model prediction, as shown in Figure 4. Agreement in luminosity is also good: 2.4 objects or $\sim$50% should be AGN with $M_B > -23$, compared to the real sample which has 3, also 50%.

In summary, the redshift and luminosity distributions of the quasars in our sample agree very well with the predictions of the model of the evolving luminosity function of Boyle et al. (1991), demonstrating consistency of the model with observations in an $M-$z regime which represents a significant extrapolation beyond the regime where it was derived.

3.1.2 Relative numbers of quasars and Seyferts

In the preceding, we have made no distinction between luminous quasars ($M_B < -23$, $H_\circ = 50$, $q_\circ = 0.5$) and lower luminosity AGNs or Seyferts. An interesting point made by Z92 is that the counts of the Seyfert galaxies are rising more steeply (with a slope of $\sim$ 0.7 in the log N vs m relation) than the more luminous objects (whose slope is $\sim$ 0.4). They note that the ratio of Seyfert to quasar counts increases from 0.1 at m$_J$ $<$ 20 to $\sim$ 0.3 at m$_J$ $<$ 21 and is $\sim$ 0.5 at m$_J$ $<$ 22. In the faintest half-magnitude bin the ratio reaches unity. In our very faint sample, the ratio of Seyfert to quasar counts also equals 1, confirming the trend noted by Z92.

3.2 Continuum properties

The continua of active galactic nuclei (AGN) are frequently characterized as power-law $f_\nu \propto \nu^\alpha$ spectra, although this is a simplification when the continuum is considered over a large range in wavelength (e.g., Neugebauer et al. 1979). For example, the continuum shape in the optical-ultraviolet region is dominated by the "blue-bump" feature which may be the signature of a hot accretion disk (Elvis et al. 1994). Since many of the quasars previously studied have been selected because they have blue continua (e.g., in ultraviolet-excess surveys), there may be biases in the statistics related to continuum shape. Hence, it is of interest to examine the continuum slopes in our sample where no such bias can exist.

The optical-UV region of quasar spectra are crowded with emission lines, Balmer continuum emission, and a number of FeII emssion features (e.g., Francis et al. 1991, hereafter F91). This makes the definition of the continuum difficult, particularly when only a restricted wavelength range (and one which varies with redshift) is available. In general, our spectra were well-fitted by power laws, but estimates of α made in this way are subject to considerable error, due to errors in the centering of any individual object among the $\sim$80 objects in our multi-slit masks. Consequently, the continuum spectral index was estimated from our $V - I$ colours (corrected for the contribution of emission lines), assuming a power law. The slopes, listed in Table 1, range from $\alpha = 0.2$ to $\alpha = -2.0$ with a mean of -1.0. The error is estimated to be $\sim \pm0.2$ in α

One of the largest and most complete surveys with which to compare our results is the Large Bright Quasar Survey (LBQS). F91 give the distribution of power-law slopes

measured in the wavelength range 1450 – 5050Å for 688 LBQS (m $\leq$ 18.85) quasars. They find a mean $\alpha = -0.32$. Francis et al. (1992) found a higher value using a principal component analysis method on a smaller subsample of the LBQS, but since the rest-frame continuum window used was very blue, the earlier analysis is better matched to our data. Interestingly, the results from our small sample span nearly the entire range in continuum slope evident in the much larger sample of F91. Half of our spectral indices are redder than -1 whereas at most 10% of those in F91 are as red as this. Furthermore, 5/6 of our spectral indices are redder than the median of the sample of F91. However, the 95% confidence interval (Gehrels 1986) for the ratio R of red-to-total objects derived from our observations is $0.36 < R < 0.996$, so that this result is not highly significant. There is no reason to believe that the survey technique employed in the LBQS would have missed the reddest (or any) quasars seen here. On the contrary, Francis et al. (1992) claim that any quasar with a continuum bluer than $\alpha \sim -2$ and/or emission lines would have been detected. Thus, although there is some indication that our sample is rather red, it does not constitute a population that would have escaped detection in the LBQS or other surveys. It should be remembered, however, that there are substantial differences in the luminosity and redshift distributions between our sample and the LBQS.

3.3 Emission-line strengths

The rest-frame equivalent widths of the three principal emission lines common to most of our spectra are listed Table 1. The equivalent widths are consistent with the means given by F91 and those compiled by Hartwick and Schade (1990), indicating once again that the quasars in our sample are not unusual. Since there has always been a lingering concern that the average emission line strengths of quasars have been biased by their detection methods, this is reassuring.

4 SUMMARY

The main goal of this paper was to compare the properties of this very faint (albeit small) sample of quasars with the properties of previously known samples. This sample was selected without any of the biases inherent in the most common survey techniques and therefore could potentially yield new insights into the population.

The surface density of AGN at $B = 23$ is 200^{+120}_{-80} deg^{-2}, the highest observed to date. This is consistent with an extrapolation of the faint counts due to Z92 and Boyle et al. (1991), and also with the lower limit found by Colless et al. (1991) based on a similar method to ours. We find that the space density of these quasars as a function of redshift and luminosity agrees very well with the predictions of the successful evolutionary model of Boyle (1991), even though our sample is deeper than any of the samples from which the model is derived.

The colours of these faint AGN are within the range defined by previously known samples and would not have escaped detection in major surveys. We find an apparent surplus of red objects compared with other studies, but the numbers are small and the significance is low. The strengths of the emission lines are entirely consistent with those found in other surveys. In summary, we find no remarkable differences between any of the properties of these faint objects and the distributions of the same properties derived from previous surveys. All our quasars would have been found by previous search techniques.

One of the quasars is in a structure consisting of at least 30 galaxies at z $\sim$ 0.985, and there is evidence that two others may be associated with groups of galaxies at a similar redshift.

REFERENCES

Boyle, B.J. 1991, in Texas-ESO/CERN symposium on Relativistic Astrophysics, Cosmology and Particle Physics, ed(s). J. Barrow, L. Mestel, and P. Thomas, Ann. N.Y. Acad. of Sci. No 647, 14

Boyle, B.J., Jones, L.R., & Shanks, T. 1991, MNRAS, 251, 482

Barcons,X., Branduardi-Raymont,G., Warwick,R.S., Fabian, A.C., Mason,K.O., McHardy, I., & Rowan-Robinson, M. 1994, MNRAS, 268, 833

Colless, M., Ellis, R.S., Taylor, K., & Shaw, G. 1991, MNRAS, 253, 686

Crampton, D.,Le Fèvre, O., Lilly, S.J., & Hammer, F. 1995, ApJ, submitted

Elvis,M., Wilkes,B., McDowell,J., Green,R., Bechtold,J., Willner,S., Oey,M., Polomski,E., & Cutri,R. 1994, ApJS, 95, 1

Francis,P.J, Hewett,P.C., Foltz,C.B., Chaffee, F.H., Weymann,R.J., & Morris,S.L. 1991, ApJ, 373, 465 (F91)

Francis,P.J, Hewett,P.C., Foltz,C.B., & Chaffee, F.H. 1992, ApJ, 398, 476

Gehrels, T. 1986, ApJ, 303, 336

Hammer, F., Crampton, D., Le Fèvre, O., Lilly, S.J., 1995, ApJ, in press

Hartwick, F.D.A. & Schade, D. 1990, ARA&A, 28, 437

Hasinger,G., Burg, R., Giacconi, R., Hartner, G., Schmidt, M., Trumper, J., & Zamorani, G. 1993 A&A, 275, 1

Hewett, P.C., & Foltz, C.B. 1994, PASP, 106, 113

Hutchings, J.B., Crampton, D. & Johnson, A. 1995, AJ, 109, 73

Koo, D.C. & Kron, R.G. 1988, ApJ, 325, 92

Le Fèvre, O., Crampton, D., Hammer, F. Lilly, S.J. & Tresse, L., 1994, ApJ, 423, L89

Le Fèvre, O., Crampton, D., Lilly, S.J., Hammer, F. & Tresse, L., 1995a, ApJ, in press

Le Fèvre, O., Lilly, S.J., Hammer, F. & Crampton, D., 1995b, in preparation

Le Févre, O., Bijaoui, A., Mathez, G., Picat, J.P., & Lelievre, G., 1986 A&A, 154, 92)

Lilly, S.J., Hammer, F., Le Fèvre, O. & Crampton, D., 1995b, ApJ, submitted

Lilly, S.J., Le Fèvre, O., Crampton, D., Hammer, F. & Tresse, L., 1995a, ApJ, submitted

Matthews, K. et al., 1994, ApJ, 420, L13

Neugebauer,G., Oke, J.B., Becklin,E.E., & Matthews,K. 1979, ApJ, 230,79

Shank,T., Georgantopoulos, I., Stewart, G.C., Pounds,K.A., Boyle, B.J., & Griffiths R.E. 1991, Nat, 353, 315

Tresse, L., Rola, C., Hammer, F. & Stasińska, G., 1994, in Wide Field Spectroscopy and the Distant Universe, eds. S. Maddox,

Webster, R.L. 1995, private communication

Zitelli, V., Mignoli, M., Zamorani, G., Marano, B., & Boyle, B.J. 1992, MNRAS, 256, 349 (Z92)

Figure 1. Flux calibrated spectra of the six quasars discovered in the CFRS survey. The strongest emission features are identified. Heavy horizontal lines indicate photometric measurements from the direct imaging in V and I. Unfortunately, the [O II] 3727Å line in the spectrum of CFRS03.0603 is coincident with the atmosperic A band, and of CFRS14.1567 with the strong [O I] 5577Å night sky emission line. Consequently their intensities are unreliable.

Figure 2. Finding charts from deep I band images of the six quasars. The images are $31''$ on a side, with N to the top, E to the left, and the quasar is in the center of each field. Other catalogued objects in the fields are identified by the last digits of their CFRS catalog numbers.

Figure 3. The cumulative surface density of quasars projected on the sky. The data represented by open circles are from the compilation of Hartwick and Schade (1990), the open triangle is from Boyle et al. (1991) the solid triangle from Z92. The faintest point (solid square) is from the present survey.

Figure 4. The redshift histogram of the CFRS quasar sample (hatched area) compared to the prediction from the evolving luminosity function model of Boyle (1991).

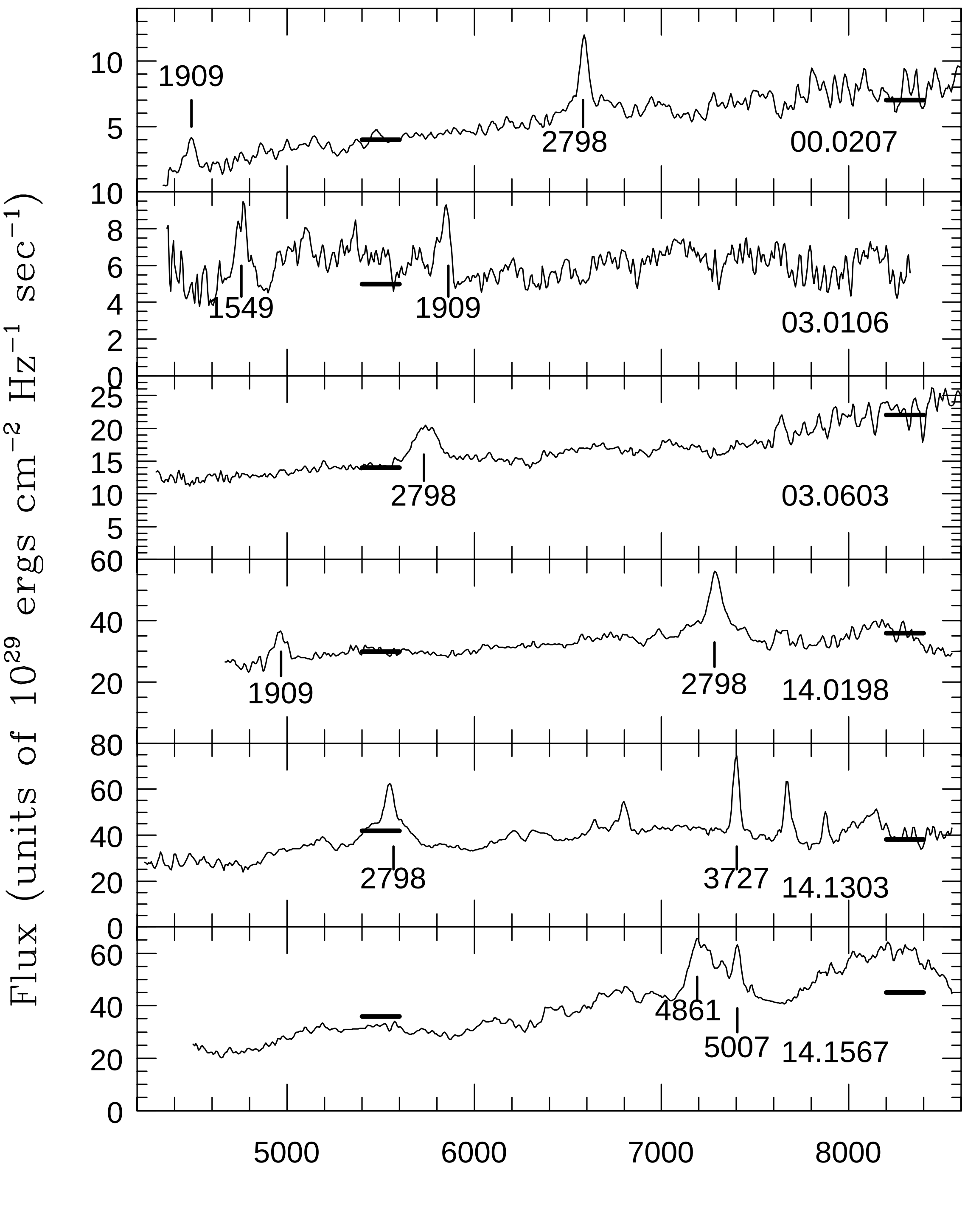

Flux (units of 10^{29} ergs cm^{-2} Hz^{-1} sec^{-1})
1909
2798
00.0207
1549
1909
03.0106
2798
03.0603
1909
2798
14.0198
2798
3727
14.1303
4861
5007
14.1567
5000
6000
7000
8000

TABLE 1

CFRS Quasar Sample

CFRS No.	RA (2000)	Dec (2000)	I_{AB} mag	z	$M_{B(AB)}$ mag	$(V-I)_{AB}$ mag	α	1549 Å	1909 Å	2798 Å
00.0207	00 02 24.52	−00 41 28.9	22.10	1.352	−22.04	0.56	−1.2	···	35	45
03.0106	03 02 23.04	+00 13 12.0	21.23	2.070	−25.21	1.03	−2.3	25	15	···
03.0603	03 02 33.14	+00 13 31.0	20.86	1.048	−23.04	0.49	−1.1	···	···	75
14.0198	14 18 16.16	+52 29 39.7	20.14	1.603	−24.72	0.17	−0.4	···	10	25
14.1303	14 17 35.88	+52 30 29.9	20.14	0.986	−23.17	−0.09	0.2	···	···	40
14.1567	14 17 24.53	+52 30 25.1	19.96	0.479	−22.03	0.25	−0.6	···	···	···

NOTE.— Absolute magnitudes assume $H_\circ = 50$ km sec^{-1} Mpc^{-1}, $q_\circ = 0.5$. The last three columns list the emission line rest-frame equivalent widths.

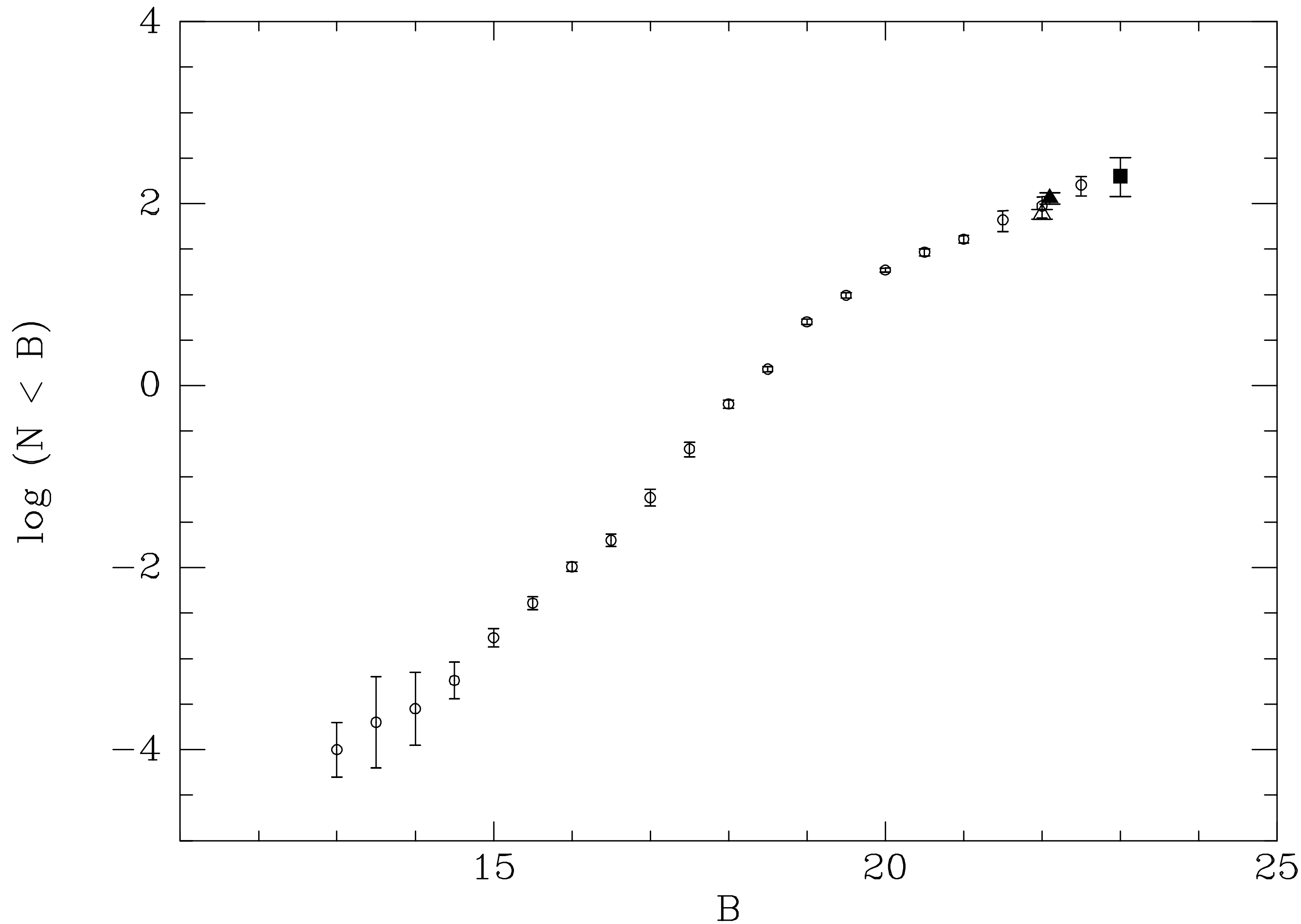

log (N < B)
4
2
0
−2
−4
15
20
25
B

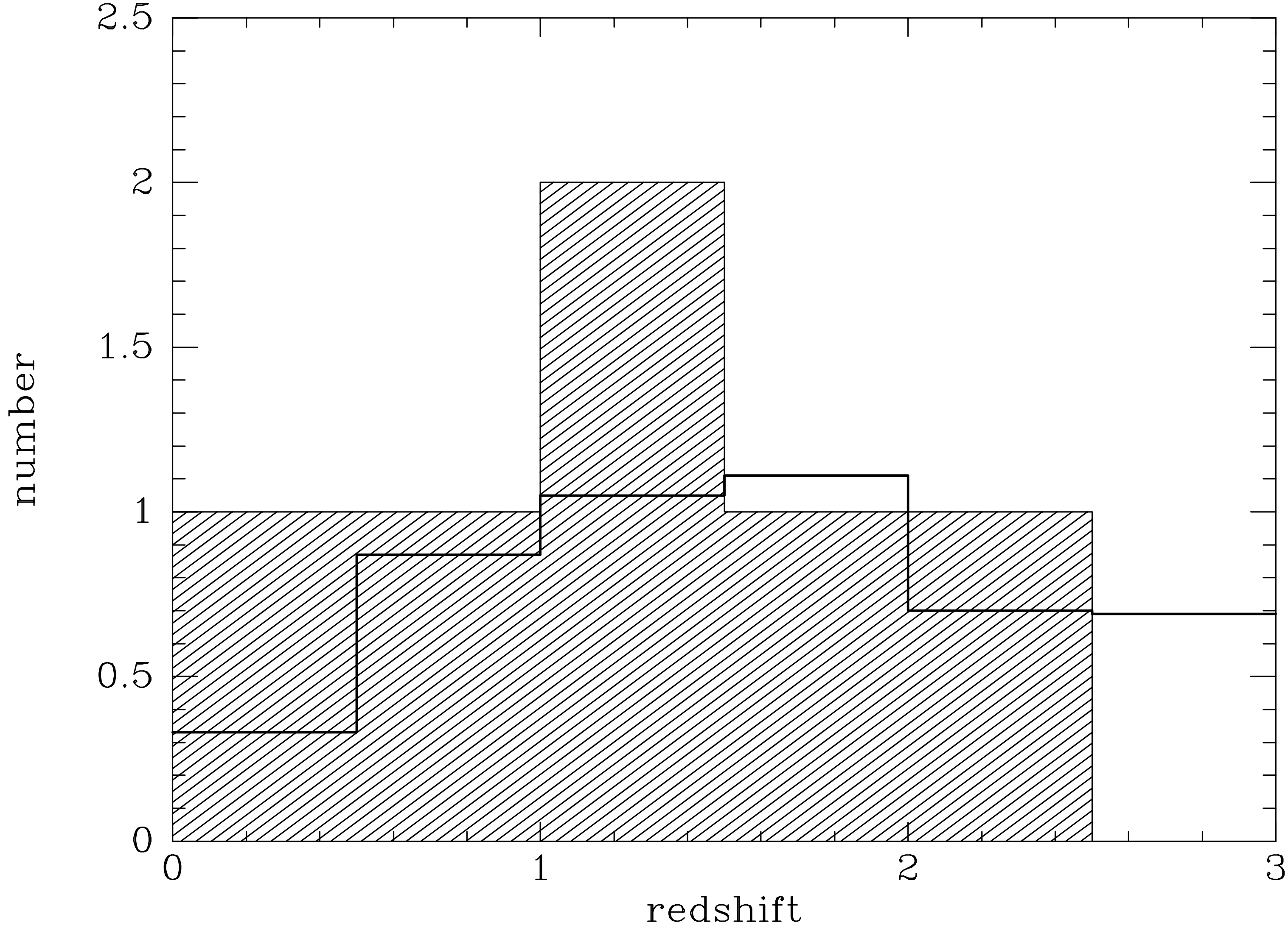

number
redshift
2.5
2
1.5
1
0.5
0
0
1
2
3